THE JOURNAL OF PHYSICAL CHEMISTRY B

Article

pubs.acs.org/JPCB

Structures, Dynamics, and Stabilities of Fully Modified Locked Nucleic Acid (β-D-LNA and α-L-LNA) Duplexes in Comparison to Pure DNA and RNA Duplexes

Gorle Suresh and U. Deva Priyakumar*

Center for Computational Natural Sciences and Bioinformatics, International Institute of Information Technology, Hyderabad 500 032, India

Supporting Information

ABSTRACT: Locked nucleic acid (LNA) is a chemical modification which introduces a $-O-CH_2-$ linkage in the furanose sugar of nucleic acids and blocks its conformation in a particular state. Two types of modifications, namely, 2′-*O*,4′-*C*-methylene-β-D-ribofuranose (β-D-LNA) and 2′-*O*,4′-*C*-methylene-α-L-ribofuranose (α-L-LNA), have been shown to yield RNA and DNA duplex-like structures, respectively. LNA modifications lead to increased melting temperatures of DNA and RNA duplexes, and have been suggested as potential therapeutic agents in antisense therapy. In this study, molecular dynamics (MD) simulations were performed on fully modified LNA duplexes and pure DNA and RNA duplexes sharing a similar sequence to investigate their structure, stabilities, and solvation properties. Both LNA duplexes undergo unwinding of the helical structure compared to the pure DNA and RNA duplexes. Though the α-LNA substituent has been proposed to mimic deoxyribose sugar in its conformational properties, the fully modified duplex was found to exhibit unique structural and dynamic properties with respect to the other three nucleic acid structures. Free energy calculations accurately capture the enhanced stabilization of the LNA duplex structures compared to DNA and RNA molecules as observed in experiments. π-stacking interaction between bases from complementary strands is shown to be one of the contributors to enhanced stabilization upon LNA substitution. A combination of two factors, namely, nature of the $-O-CH_2-$ linkage in the LNAs vs their absence in the pure duplexes and similar conformations of the sugar rings in DNA and α-LNA vs the other two, is suggested to contribute to the stark differences among the four duplexes studied here in terms of their structural, dynamic, and energetic properties.

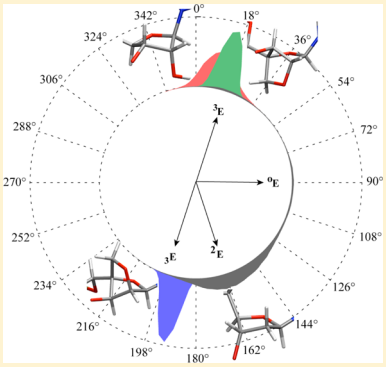

INTRODUCTION

Chemically modified nucleic acids have potential applications in modern nucleic-acid-based therapies.[1,2] Certain chemical modifications to the backbone of DNA and RNA duplex structures have been shown to increase their stability, and they also have been shown to resist nuclease activity.[3,4] In antisense therapy, maturation of m-RNAs is typically blocked when a chemically modified antisense strand binds to them due to which the translation process cannot proceed further.[5,6] This necessitates a search for suitable antisense oligonucleotides comprising chemical modifications that attribute high stability to the duplex. Several experimental and theoretical studies have suggested that chemical modifications can be introduced at the base, sugar, and backbone moieties in the nucleic acid strands.[7−18] Some of the well-studied modifications to the sugar moiety include 2′-*O*-alkyl,[7] 2′-*O*,4′-*C*-methylene (LNA),[8−10] arabinonucleic acids (ANA),[11] 2′-*F*-arabinonucleic acids (2′-*F*-ANA),[12] cyclohexyl nucleic acids (CeNA),[13] and 2′-fluoro substitutions;[14] the most common variations to the backbone include peptide nucleic acids (PNA),[15] phosphoroamidate,[7] and 2′-*S*-phosporoamidate;[16] and some of the modifications introduced in the base moiety are C5-propynyl[17] and 5-(*N*-aminohexyl) carbamoyl substitutions.[18]

DNA−RNA hybrid duplexes exhibit both B- and A-type nucleic acid properties, and are readily degraded by nucleases.[19−26] The primary aim of the above-mentioned strategies is to identify modifications that will make the duplex behave more like a typical A-type nucleic acid which is expected to resist nuclease activity. In this context, locked nucleic acids (LNA) that increase the stability of duplex molecules in general have been extensively studied.[8−10] In LNAs, the chemical modification $-O-CH_2-$ group is introduced in the sugar moiety which connects the C2′ and C4′ atoms (Scheme 1) and blocks the sugar ring in a single conformational state. This chemical modification in nucleic acid strands has been shown to increase their affinity toward the complementary DNA and RNA strands and results in an increase of their melting temperatures.[8] Because of this high affinity, the LNA modified nucleic acids have found many applications in several important areas in biotechnology and molecular biology.[27,28] These have also found potential applications in DNAzymes,[29] molecular becons,[30] siRNA approaches,[31] and antisense therapy.[32] LNA modified duplexes are also used as probes in RNA *in situ*

Received: February 14, 2013
Revised: March 29, 2013
Published: April 25, 2013

Scheme 1. Structures of the Sugar Moieties of DNA, RNA, α-LNA, and β-LNA Duplexes and Their Three-Dimensional Structural Representations

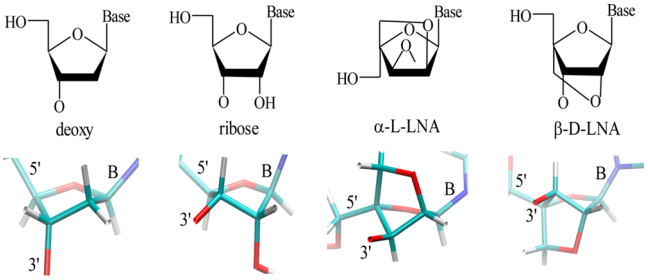

hybridization[33,34] and as aptamers for NF-κB transcription factor.[35] It is also observed experimentally that the LNA modified antisense oligonucleotides inhibit HIV-I expression.[36] In recent studies, the LNA modification has been utilized in retaining or improving the ligand−aptamer binding in Hammerhead ribozyme[37] and G-quadruplex thrombin aptamer.[38]

Previous studies have reported that the modification 2′-*O*,4′-*C*-methylene-β-D-ribofuranose (β-LNA) locks the sugar conformation (^{3}E) similar to ribose sugar and the corresponding α-enantiomer 2′-*O*,4′-*C*-methylene-α-L-ribofuranose (α-LNA) locks the sugar conformation ($_3$E) similar to deoxyribose sugar (Scheme 1). Hence, the two modifications, β-LNA and α-LNA, are considered as RNA and DNA mimics, respectively.[39,40] This means that the full β-LNA and α-LNA modifications in nucleic acid duplexes result in typical A- and B-type duplexes similar to A-RNA and B-DNA duplexes, respectively. However, the recently solved crystal structure of a full β-LNA double helix[41] along with a previous computational study[42] revealed that the β-LNA and RNA duplexes differ from each other in a number of structural, dynamic, and energetic properties. The LNA duplex has decreased values of roll, twist, and propeller twist than A-RNA duplex which resulted in widening of the major groove. An empty tunnel is observed in LNA duplex which runs through the center of the helix along the helical axis due to shift in their base pairs. The structural properties observed in the LNA duplex showed that its geometry is reasonably different from a typical A-type duplex. NMR experimental studies showed that the introduction of α-LNA monomers in RNA duplex changes the conformation into A/B-type[39] and in DNA duplex preserves its B-type conformation.[43] There are no studies concerning the structural and energetic properties of fully substituted α-LNA duplexes. As mentioned above, an X-ray crystal structure of a full β-LNA duplex has been published recently.[41] In the present paper, an attempt is made to investigate the structural, dynamic, and energetic properties of fully modified LNA duplexes (α-LNA and β-LNA) and how they compare to the corresponding pure DNA and RNA duplexes using MD simulations.

COMPUTATIONAL METHODS

Simulation Setup. MD simulations were performed using the CHARMM36 all atom nucleic acid force field[44−46] with the NAMD program.[47] Simulations were performed corresponding to two LNA modified (α-LNA and β-LNA) duplexes and two ideal (A-RNA and B-DNA) duplexes sharing a similar nonamer sequence (CTGATATGC). The thymine bases in the RNA and LNA modified duplexes were replaced by uracil bases in accordance with experiments.[39,41] Starting structures for α-LNA and β-LNA duplexes were canonical B- and A-type conformations, and duplex modeling was done using the CHARMM biomolecular simulation program.[48] The partial charges and corresponding force field parameters for LNA modification were taken from the study of Pande et al.[42] Initially, these systems were minimized using 200 steepest descent (SD) steps following which these systems were immersed in a pre-equilibrated water box with dimensions of 48 Å × 38 Å × 38 Å. The overlapping water molecules with the solute were removed on the basis of a cutoff distance of 1.8 Å, and these systems were neutralized by placing sodium ions randomly. These systems were then minimized using SD and adopted basis Newton−Rapson (ABNR) methods (500 steps with each of the methods), followed by 100 ps MD simulation by having a weak harmonic restraint of 5 kcal/mol/Å^2 on the heavy atoms of nucleic acid duplexes. The covalent bonds involving hydrogen atoms were constrained using the SHAKE algorithm,[49] which allowed the use of 2 fs as an integration time step during all the simulations. The modified TIP3P water model was used to model an explicit solvent environment.[50] Periodic boundary conditions via the CRYSTAL module implemented in CHARMM were used.[51] The particle mesh Ewald (PME) summation method was used to treat long-range electrostatic interactions.[52,53] A force smooth switch function was set up from 10 to 12 Å which helped in truncating the Lennard-Jones (LJ) interactions at 12 Å.[54] The temperature and pressure of the systems were maintained at 300 K and 1 atm by employing a Nosé−Hoover thermostat[55] and Langevin piston,[56] respectively. Using the NAMD program following a similar protocol described above, 22 ns long production simulations were performed for all the systems in the NPT ensemble. A weak harmonic constraint with a force constant of 4 kcal/mol/Å^2 was applied on hydrogen bonds of terminal base pairs to prevent fraying during the simulations.[42] The coordinates were saved every 5 ps during the simulations and used for analysis.

Analysis of the Trajectories. All the analyses of the trajectories were done using the CHARMM biomolecular simulation[48] and Curves+[57] programs along with scripts written in the lab. The images of structures depicted in Figure 1 were

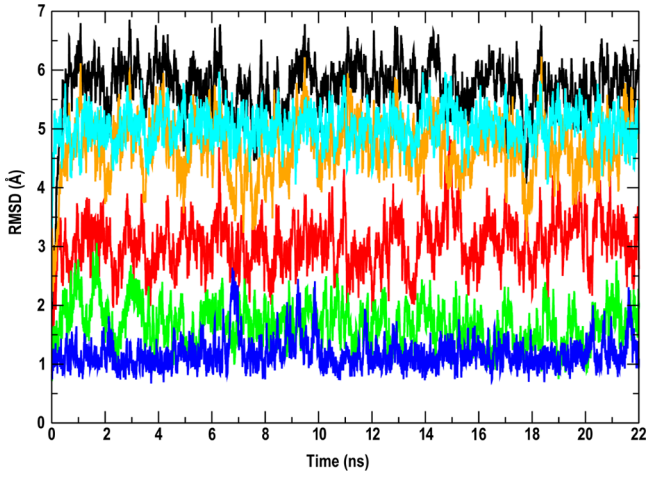

Figure 1. Time series of the RMSD values of α-LNA with respect to B- (black) and A-type (orange) and of β-LNA with respect to B- (cyan) and A-type (red). RMSDs of the DNA (green) and RNA (blue) duplexes with respect to their initial structures are also given for comparison.

dx.doi.org/10.1021/jp4016068 | J. Phys. Chem. B 2013, 117, 5556−5564

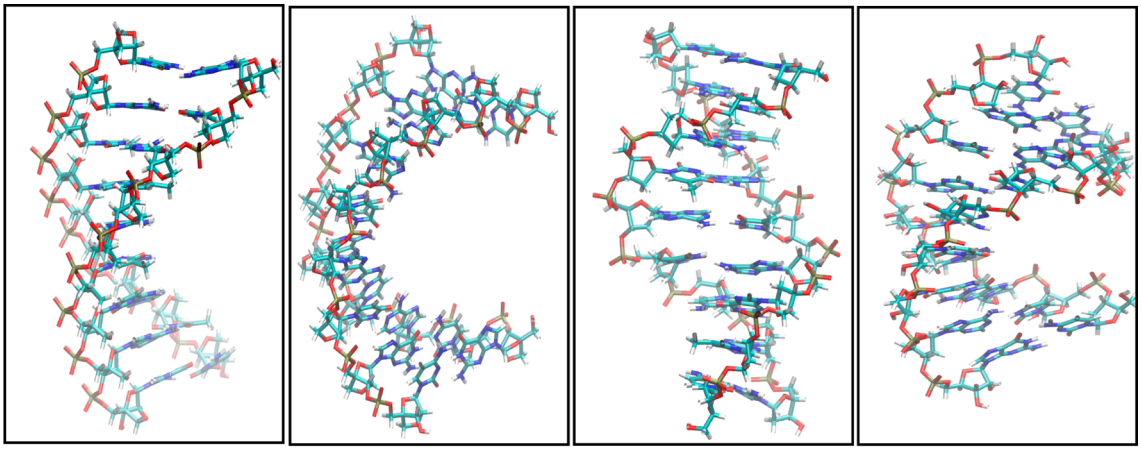

Figure 2. Snapshots of the structures of (a) α-LNA, (b) β-LNA, (c) pure DNA, and (d) pure RNA duplexes obtained after the 22 ns MD simulations.

generated using the Visual Molecular Dynamics (VMD) program.[58] All the analyses presented here are based on the final 18 ns simulation trajectories. The translation and rotational motions were removed by superimposing all the frames in the trajectories corresponding to non-hydrogen atoms with their initial structure. The root-mean-square deviations (RMSD) were calculated by least-squares fitting of all the non-hydrogen atoms to their starting structure. The interstrand phosphate−phosphate distances were calculated by considering interatomic distances between phosphates present in the complementary strands, and the intrastrand phosphate−phosphate distances were calculated as the interatomic distances between phosphates present in the same strand. Stacking interaction energies were calculated using the INTER command in the CHARMM program taking into account only the nonbonded LJ terms. Interstrand stacking interaction is the interaction energy of a given base with the bases adjacent to the WC base pair partner in the complementary strand. Intrastrand stacking interaction is the interaction energy of a given base with its adjacent bases in the same strand.[22] To examine the solvation properties around the duplexes, solvent accessible surface area (SASA) calculation was done using a probe particle with radius 1.4 Å. The SASA values were calculated around the minor (N3, O2, H21, and H22) and major (O6, N7, O4, H61, and H62) grooves and backbone oxygens (O1P, O2P, O3′, and O5′). Entropy calculations were done using quasiharmonic analysis via the VIBRAN module implemented in CHARMM.[59] Hydration numbers were calculated by counting the water molecules whose oxygen atom is present within 3.5 Å from the N or O atoms of the duplex.

Free Energy Calculations. Molecular mechanics with the generalized Born-surface area method (MM-GBSA) was employed to calculate the binding free energies.[60] The binding free energy of a duplex is calculated as the difference in the free energies of the duplex and the sum of the free energies of the individual strands as explained below. This method uses molecular mechanical energy, solvation energy, and entropy of the solute to calculate binding free energies.[61] In general, the binding free energy of the duplex can be calculated as

$$\Delta G_{bind} = G_{duplex} - G_{strand1} - G_{strand2}$$

where G_{duplex}, $G_{strand1}$, and $G_{strand2}$ represent the free energies of the duplex and individual strands present in the duplex. The free energies of the individual strands have been estimated using the same trajectories as that of the duplex, thus ignoring the expected effect of single strands sampling a larger conformational space. Since the primary interest here is to examine the relative free energy differences that compare the four duplex structures, this approach is expected to be adequate to get the qualitative trends correct.[62,63] The free energy of each of the three can be estimated using the following equation

$$G = E_{MM} + G_{solv} - TS_{MM}$$

where G represents the free energy, E_{MM} represents the molecular mechanical energy, G_{solv} is the solvation free energy, T is the absolute temperature, and S_{MM} is the entropy of the system. E_{MM} is the sum of all the energy terms in the force field equation, and the solvation free energy has contributions from electrostatic solvation energy (G_{polar}) and nonpolar solvation energy ($G_{nonpolar}$).

$$G_{solv} = G_{polar} + G_{nonpolar}$$

The electrostatic contribution (polar) to the solvation free energy was estimated by using the generalized-Born molecular volume (GBMV) method, and the nonpolar contribution toward solvation free energy was estimated as $G_{nonpolar} = \gamma SASA$, where $\gamma = 0.0072$ kcal/mol/Å^2.[64,65]

RESULTS AND DISCUSSION

Overall Structure and Dynamics. The structures obtained using the MD simulations were compared with the initial structures using the root-mean-square-deviation (RMSD) calculations (Figure 1). Additionally, RMSD values for the LNA duplexes were also calculated with respect to canonical B- and A-form duplexes. The RMSD values calculated for all of the trajectories from the MD simulations indicate sufficient equilibration well within the first 4 ns. Both α- and β-LNAs undergo rapid transition from their respective initial structures modeled as typical B- and A-form duplexes, respectively, to stable structures during the first ns of the simulation. Figure 2 depicts the structures of the four duplexes after the 22 ns MD simulations. Visual inspection of the snapshots indicates similar structures for both the α- and β-LNA duplexes with both of

dx.doi.org/10.1021/jp4016068 | J. Phys. Chem. B 2013, 117, 5556−5564

them undergoing unwinding of the helix compared to the DNA and RNA molecules. This is in contrast to the previous suggestions that α-LNA adopts a conformation similar to a typical B-type nucleic acid, since the chemical modification locks the sugar ring in the $_3$E conformation. Structures of the LNA duplexes obtained in the current study are similar to those observed by Forster et al. in an X-ray crystallographic study[41] and by Pande et al. in an MD simulation study[42] on β-LNA duplexes. Though similar helical unwinding was observed for both of the LNA molecules, closer examination revealed significantly different helical and other conformational properties (see below). To further understand the nature of LNA duplexes, their structures were compared with typical A and B conformations (Figure 1). The β-LNA duplex exhibits low RMSD values with respect to the A-form than the B-form models, indicating A-like structure for the β-LNA duplex, which is in good agreement with previous studies.[41] On the other hand, the RMSD values obtained for the α-LNA with respect to typical A- and B-form duplexes (4.71 and 5.72 Å, respectively) indicate that the overall structure does not resemble either of the conformational states. Interestingly, α-LNA exhibits a lower deviation with respect to the A-form than the B-form irrespective of the fact that this substitution locks the sugar in the $_3$E conformation like in the DNA. The flexibilities of these duplex structures examined using root-mean-square-fluctuation calculations indicate similar behavior both at the level of the base and the backbone (Table S1, Supporting Information).

Stabilities of the LNA Duplexes Compared to the Pure DNA and RNA Duplexes. Previous studies have suggested that LNA modifications lead to an increase in the melting temperatures of the nucleic acid duplexes.[41] This section examines the stability of the four nucleic acid molecules by calculating certain energetic factors including free energy estimates. The integrity of the base pair interactions in the duplex structures was characterized by calculating the probability distributions corresponding to all the N1(purine)−N3(pyrimidine) distances of the Watson−Crick base pairs (Figure S1, Supporting Information) and the interaction energies between the individual bases comprising each base pair (Table S2, Supporting Information). In all the probability distributions, peaks at 3 Å and near zero probabilities corresponding to distances more than 4 Å indicate stable Watson−Crick base paired states. Similarly, all the interaction energies are comparable to each other, and with respect to the interaction energies obtained for respective optimized base pairs. It has been previously suggested that the LNA modified backbone orients in such a way that the stacking between base pairs is enhanced.[39] To examine the effect of LNA substitutions on the extent of stacking in these duplexes, stacking interactions (see the Computational Methods section) between a given base with its neighboring bases present in the same strand and in the complementary strand were calculated (Table 1). More favorable interstrand interaction energies are expected to enhance the overall stability of the nucleic acid duplex. The data presented in Table 1 clearly show that the interstrand interaction energies in the LNA duplexes are more favorable than those in the pure duplexes, indicating enhanced stabilization upon LNA modification. However, the intrastrand interaction energies are more stabilizing in the pure duplexes than in the modified duplexes. Because of the presence of a bulky methylene group, the intrabase stacking interactions seem to have reduced, whereas there is an increase in the stacking interactions with other bases in the complementary strand which results in helical unwinding in order to stabilize the overall LNA duplex. The extents of stabilization because of the interstrand interactions in the α- and β-LNA modifications are comparable (−5.3 and −5.2 kcal/mol, respectively). Previous studies have indicated that the melting temperatures of unmodified DNA and RNA duplexes increase by about 2−10 °C for every single incorporation of α-/β-LNA modification.[8,39] Free energy changes with respect to the formation of a duplex from individual strands were calculated using the MM-GBSA method to further estimate the stabilities of these nucleic acids (Table 2). The estimates of the free energy changes with and without the contribution of the entropy of the solute are given in the table. The individual components of the free energy changes along with the errors are presented in Table S3 in the Supporting Information. In agreement with the experimental studies,[39,41,66] the free energy differences are found to be more favorable for both of the LNA duplexes compared to the corresponding pure DNA and RNA molecules, indicating a high stability of the former. The two LNA modifications which are differentiable with respect to their isomerization exhibit similar stabilities. It has to be noted that the free energy estimates presented here are approximate, and only the qualitative trends are used for evaluating the relative stabilities of the nucleic acids. Within the approximations used here, good agreement with the experimental data in terms of the qualitative trends was observed.[39,41,66] The following section examines the conformational properties of the duplexes considered here in detail.

Table 1. Average Intra- and Interstacking Interaction Energies (kcal/mol) Calculated for the Four Duplexes

duplex	intrastrand	interstrand	overall
α-LNA	−8.70	−5.32	−14.01
β-LNA	−8.21	−5.24	−13.46
DNA	−11.82	−3.66	−15.48
RNA	−9.89	−4.37	−14.26

Table 2. Binding Free Energies (in kcal/mol) for All the Duplexes Calculated Using the MM-GBSA Method[a]

duplex	ΔG_1	ΔG_2
α-LNA	−110.72	−87.50
β-LNA	−110.23	−87.67
DNA	−91.89	−67.92
RNA	−99.72	−77.91

[a] ΔG_1 and ΔG_2 are binding free energies that were calculated without and with entropic contribution, respectively.

Conformational Properties of the Backbone. Conformational preferences of the backbone were investigated by calculating the phosphodiester backbone dihedral angles and pseudorotation angles of the sugar rings. These geometric parameters are capable of readily differentiating different forms of nucleic acids including the A- and the B-forms. The probability distributions corresponding to the phosphodiester dihedral angles (α (O3′−P−O5′−C5′), β (P−O5′−C5′−C4′), γ (O5′−C5′−C4′−C3′), ε (C4′−C3′−O3′−P), ζ (C3′−O3′−P−O5′), and χ (C1′−N9 for purines and C1′−N1 for pyrimidines)) obtained for the four duplexes are depicted in Figure 3. The dihedral angles calculated for the X-ray structure of a β-LNA duplex[41] are also given for comparison. The pure

dx.doi.org/10.1021/jp4016068 | J. Phys. Chem. B 2013, 117, 5556−5564

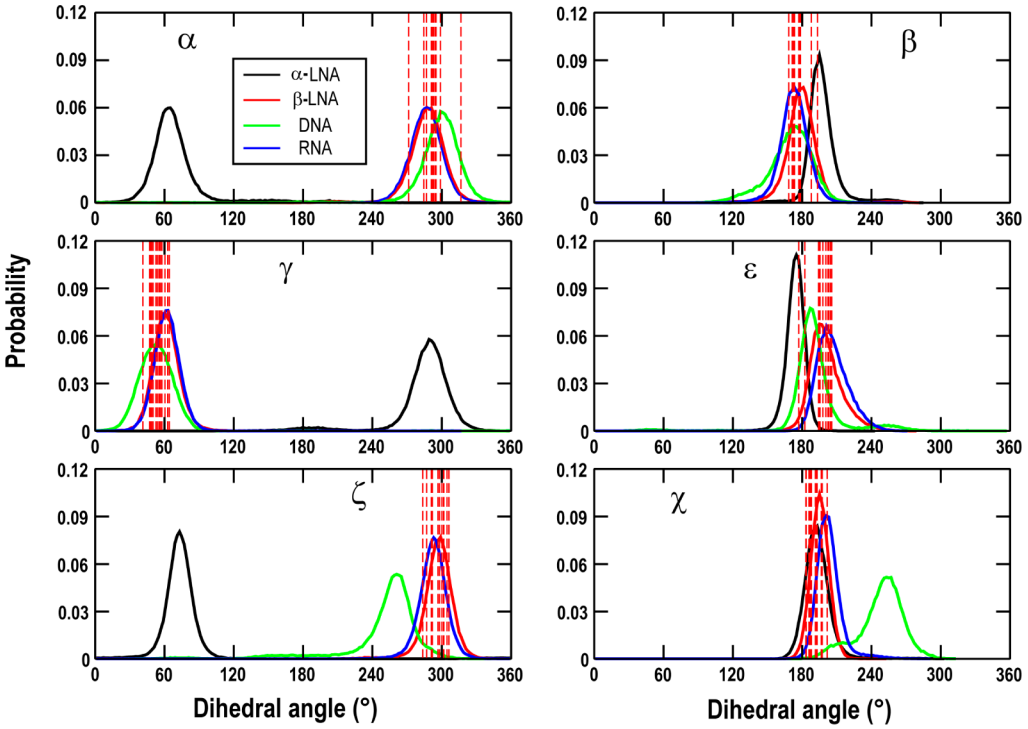

Figure 3. Probability distributions of phosphodiester backbone and glycosidic bond dihedral angles corresponding to all the duplexes studied. The dihedral angles obtained from the X-ray structure of a *β*-LNA duplex are represented as red spikes for comparison.

DNA and RNA duplexes exhibit B- and A-form characteristics, respectively, and the distributions obtained for these molecules are consistent with previous studies.[22] Excellent agreement between the calculated probability distributions and the available experimental data for the *β*-LNA duplex is observed. The distributions of the dihedral angles show that the *β*-LNA duplex samples a conformation space similar to that of a typical A-type duplex. Extensive overlap between the distributions computed for *β*-LNA and RNA was observed, indicating almost identical structures in terms of the conformation of the backbone of the two duplexes. However, *α*-LNA displays conformational characteristics that are completely different from both A- and B-form duplexes. The only probability distribution of the *α*-LNA that is similar to that of either A- or B-type duplex is the one corresponding to the glycosidic dihedral angle, *χ*. Surprisingly, even in this case, it exhibits A-form and not B-form structural characteristics. As suggested by previous studies, the *β*-LNA modification locks the sugar in the ^{3}E conformation, whereas the *α*-LNA modification confines the sugar in the $_{3}$E conformation.[8,39] While the sugars in *α*-LNA sample the $_{3}$E conformational region, it is considered as N-type because the sugar is in the L-form.[66] Probability distributions for the pseudorotation angles of all the five-membered rings were calculated to investigate the conformational preferences of the sugar moieties (Figure 4). The sugar rings of the pure RNA duplex sample in the ^{3}E region, and the DNA duplex samples the ^{2}E region in addition to minor sampling of the ^{3}E and ^{O}E regions as expected. The conformations of the modified five-membered rings of the *β*-LNA duplex were observed to be very similar to that of the RNA. However, similar to the phosphodiester torsion angles, *α*-LNA samples a conformational space that is very different from the other three duplexes but close to B-DNA. Sampling of the $_{3}$E conformation by the five-membered rings of the *α*-LNA further confirms a

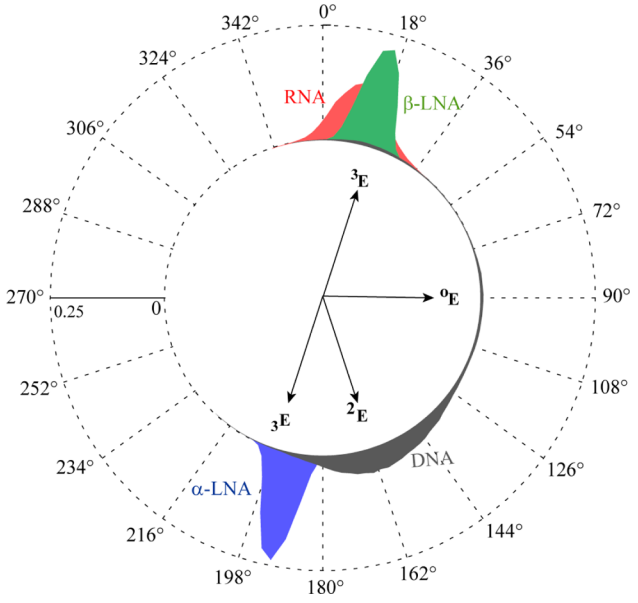

Figure 4. Probability distributions of the pseudorotation angles of the sugar rings computed for the four duplexes considered in the present study.

completely different nucleic acid form. Understandably, the distributions of the pseudorotation angles of both the LNA duplexes are comparatively narrow because of the bicyclic nature of the ring. Considerable differences in the conformational properties of the backbones of the LNA modified duplexes and overall unwinding of the helical structures seem to contribute to interesting trends in the end-to-end distances, and interphosphate distances. While LNA modifications seem to affect the interstrand phosphate distances (Figure S2a, Supporting Information), the conformation of the sugar ring

dx.doi.org/10.1021/jp4016068 | J. Phys. Chem. B 2013, 117, 5556−5564

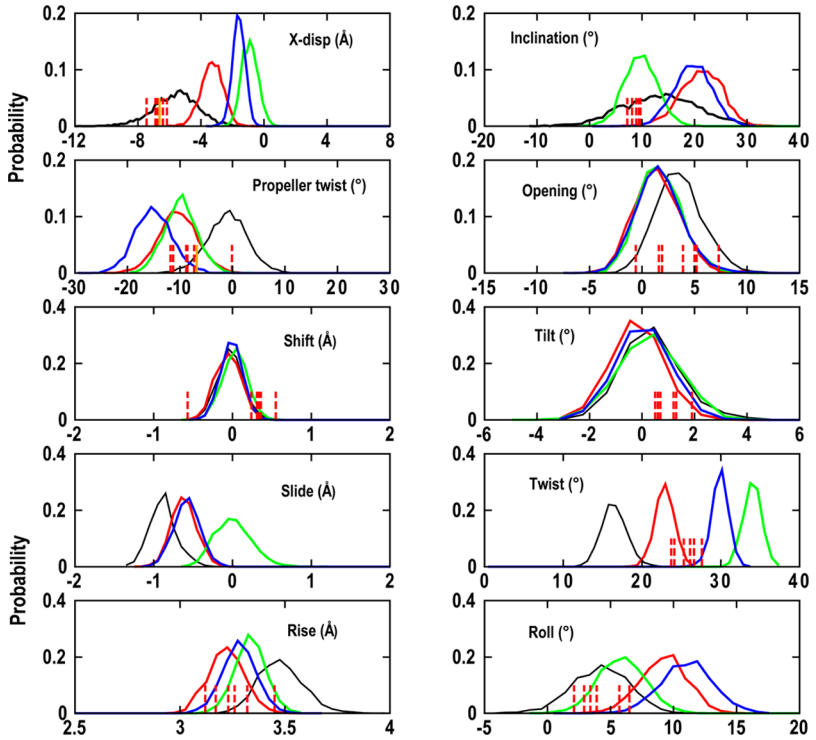

Figure 5. Probability distributions of *X*-displacement, inclination, propeller twist, base pair opening angle, and local translational and rotational parameters calculated for α-LNA (black), β-LNA (red), DNA (green), and RNA (blue). The dotted red spikes are the values calculated from the X-ray structure of a β-LNA duplex.

seems to be the determinant of the intrastrand phosphate distances (Figure S2b and c, Supporting Information). The end−end distance of the duplexes, calculated as the distance between center of masses of the terminal base pairs, shows that α-LNA is elongated compared to β-LNA and the pure duplexes (Figure S3, Supporting Information). These results further substantiate our earlier observation that the structure of the α-LNA duplex is distinct from ideal A- and B-type duplexes and β-LNA duplex. The structural properties of the nucleic acid duplexes were further examined by calculating the helical properties as given in the following section.

Helical Parameters. Selected helical geometric properties and base pair step parameters which provide detailed information on the orientation of the base pairs with respect to the helical axis and neighboring base pairs respectively are presented in Figure 5. Plots of values obtained for every base pair step corresponding to some of these helical parameters are provided in the Supporting Information (Figure S4). Both the LNA incorporated duplexes have higher *X*-displacement values compared to the pure duplexes, which indicates that the base pairs have translated toward the minor groove side. However, the inclination values are lower for the two duplexes with S-type sugars (α-LNA and DNA) than the other two with N-type sugars (β-LNA and RNA), indicating that the base pairs of the latter are tilted with respect to the helical axis more than those of the former. However, α-LNA exhibits a broad probability distribution overlapping with all the other three duplexes. Maximum probabilities corresponding to values of zero or close to zero for the intra-base-pair parameters (propeller twist and opening angles) indicate stable WC base pairing of all the bases in the duplex. Interestingly, α-LNA shows the lowest propeller twist values among all the duplexes, and the distribution is centered about 0°. Similar values for the base pair step parameters, shift and tilt, were observed for all the duplexes. However, the α-LNA duplex shows lower values of slide and higher values of rise compared to the others. The helical unwinding of the LNA incorporated duplexes discussed above is clearly reflected in the twist values given in Figure 5. Both the duplexes, especially the α-LNA, exhibit lower values of twist compared to the pure duplexes, resulting in high helical unwinding. The twist value of α-LNA duplex is even smaller than other chemically modified PNA[67] and GNA[68] duplexes reported in previous studies. The subtle deviations in the base step parameters seem to have facilitated widening of the major groove of LNA duplexes and consequently narrowing of their minor groove width. The α-LNA duplex is observed to have a very narrow minor groove width (Figure 6). The minor groove of the β-LNA is lower than that of the pure RNA duplex but similar to DNA−RNA hybrid duplexes.[20,22]

Solvation Properties. Hydration around nucleic acids plays an important role in their stability and function. The differences in the solvation patterns around certain regions among the four duplexes were examined by calculating the SASA values and hydration numbers (Table 3). Hydration number is defined as the number of water molecules whose oxygen atoms are within 3.5 Å of N/O atoms of the duplex. Comparison of the SASA values and hydration numbers show that the oxygen atoms of the phosphodiester moieties are well exposed in the S-type conformation (α-LNA and DNA) than in the N-type conformation (β-LNA and RNA). Notably, the phosphodiester oxygen atoms in α-LNA are better solvated compared to even the DNA duplex. The SASA values and the hydration numbers of the major and minor grooves of the structures indicate higher solvation in the RNA and LNAs compared to the DNA duplex. The hydration numbers obtained in this study are slightly different from those obtained

dx.doi.org/10.1021/jp4016068 | J. Phys. Chem. B 2013, 117, 5556−5564

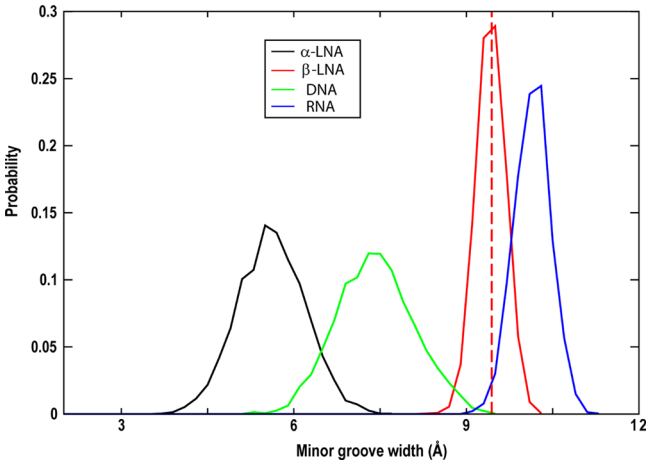

Figure 6. Probability distributions of minor groove widths of the duplexes. The minor groove width value corresponding to the β-LNA duplex characterized by X-ray experiments is given by a dotted line.

by Pande and Nilsson possibly because of the different criteria used.[42] Previously, it has been proposed that the O2′ atom present in β-LNA facilitates its minor groove hydration similar to RNA and the solvation pattern is comparable with the RNA minor groove hydration. The O2′ atom of the $-O-CH_2-$ linkage is present at the brim of the minor groove in β-LNA and the major groove in α-LNA duplexes.[66] The bases in B-type duplexes are better exposed to solvent than A-type duplexes. As indicated by the SASA values and hydration numbers, the major groove in α-LNA duplex has a better solvation pattern compared to RNA duplex because of the presence of an O2′ atom.

CONCLUSIONS

Explicit MD simulations were performed on nucleic acid duplexes with fully incorporated locked nucleic acid (LNA) modifications to examine their structural and energetic properties, and to understand how they compare with DNA and RNA duplexes. Out of eight possible isomers for LNA modification, two of the common ones, namely, α- and β-LNA, which were suggested to mimic DNA and RNA, respectively, are studied here. MD simulations resulted in stable structures, and the β-LNA duplex was found to resemble the overall structure of a typical A-form nucleic acid, whereas the α-LNA duplex significantly differs from both A- and B-form nucleic acids. However, both of the LNA duplexes were found to undergo unwinding that is reflected in the analysis of the helical properties and other geometric parameters. This is in contrast to previous suggestions that α-LNA substitutions result in DNA-like structures, since their sugar rings are conformationally similar to each other. Very good agreement between the current results and earlier experimental/computational studies on β-LNA duplex was observed.[41,42] Free energy calculations suggest that chemical modifications involving either α-LNA or β-LNA impart significant stability to the structures compared to pure duplexes, an observation reported by previous experiments.[8,39,41] One of the factors contributing to high stability of the duplexes is identified as the enhanced interstrand stacking interactions. The presence of O2′ in the LNA molecules results in better hydration of the backbone similar to RNA duplexes. All geometric parameters such as backbone conformations, sugar ring conformations, and helical properties indicate that α-LNA exhibits interesting structural and dynamic properties in addition to enhanced stability. Thus, the unique properties displayed by α-LNA duplex may lead to better resistivity toward nuclease activity, which makes it a potential candidate to be explored as an antisense therapeutic agent. A systematic study of incremental modification of α- and β-LNA moieties in nucleic acid duplexes and its effect on their structures/stabilities is currently being carried out.

ASSOCIATED CONTENT

Supporting Information

Tables of RMSF, base pair interaction energies and average values of individual components of binding free energy calculations, and figures of probability distributions of hydrogen bond lengths in the base pairs, end−end distances, phosphate−phosphate distances, and select helical parameters. This material is available free of charge via the Internet at http://pubs.acs.org.

AUTHOR INFORMATION

Corresponding Author

*E-mail: deva@iiit.ac.in. Phone: +91-40-6653 1161. Fax: +91-40-6653 1413.

Notes

The authors declare no competing financial interest.

ACKNOWLEDGMENTS

Department of Atomic Energy (Govt. of India) is acknowledged for financial assistance. G.S. thanks Council of Scientific and Industrial Research (CSIR), India, for a research fellowship.

Table 3. Solvent Accessible Surface Area (SASA) Values (Å^2) and Hydration Numbers around Different Regions of the Duplexes

duplex	overall	bases	phosphodiester oxygens	minor groove	major groove
			SASA		
α-LNA	2895.4 ± 4.8	686.3 ± 0.9	1263.7 ± 0.8	92.2 ± 0.8	137.3 ± 1.0
β-LNA	2729.9 ± 2.2	493.7 ± 0.8	1020.2 ± 2.2	90.6 ± 1.0	163.7 ± 1.9
DNA	2603.8 ± 3.2	501.6 ± 1.2	1142.0 ± 3.2	83.7 ± 0.7	76.0 ± 0.5
RNA	2536.1 ± 3.5	395.9 ± 0.8	1068.7 ± 1.5	91.8 ± 0.6	123.9 ± 1.4
			Hydration Number		
α-LNA	170.8 ± 4.7	76.8 ± 1.0	107.3 ± 3.3	15.8 ± 0.6	21.5 ± 0.3
β-LNA	165.4 ± 2.6	64.6 ± 0.5	90.3 ± 2.4	16.0 ± 0.3	23.1 ± 0.3
DNA	151.1 ± 4.4	66.6 ± 0.3	101.5 ± 4.1	15.0 ± 0.1	17.2 ± 0.1
RNA	161.3 ± 4.2	56.5 ± 0.7	95.7 ± 3.4	17.1 ± 0.5	20.3 ± 0.3

REFERENCES

(1) Uhlmann, E.; Peyman, A. Antisense Oligonucleotides: a New Therapeutic Principle. *Chem. Rev.* **1990**, *90*, 543−584.
(2) Helene, C.; Toulme, J. J. Specific Regulation of Gene Expression by Antisense, Sense and Antigene Nucleic Acids. *Biochem. Biophys. Acta* **1990**, *1049*, 99−125.
(3) Dias, N.; Stein, C. A. Antisense Oligonucleotides: Basic Concepts and Mechanisms. *Mol. Cancer Ther.* **2002**, *1*, 347−355.
(4) Freier, S. M.; Altmann, K. H. The Ups and Downs of Nucleic Acid Duplex Stability: Structure Stability Studies on Chemically Modified DNA:RNA Duplexes. *Nucleic Acids Res.* **1997**, *25*, 4429−4443.
(5) Dove, A. Antisense and Sensibility. *Nat. Biotechnol.* **2002**, *20*, 121−124.
(6) Kurreck, J. Antisense Technologies: Improvement through Novel Chemical Modifications. *Eur. J. Biochem.* **2003**, *270*, 1628−1644.
(7) Manoharan, M. 2′-Carbohydrate Modifications in Antisense Oligonucleotide Therapy: Importance of Conformation, Configuration and Conjugation. *Biochim. Biophys. Acta* **1999**, *1489*, 117−130.
(8) Vester, B.; Wengel, J. LNA (Locked Nucleic Acid): High-Affinity Targeting of Complementary RNA and DNA. *Biochemistry* **2004**, *43*, 13233−13241.
(9) Braasch, D. A.; Corey, D. R. Locked Nucleic Acid (LNA): Fine-Tuning the Recognition of DNA and RNA. *Chem. Biol.* **2001**, *8*, 1−7.
(10) Petersen, M.; Wengel, J. LNA: a Versatile Tool for Therapeutics and Genomics. *Trends Biotechnol.* **2003**, *21*, 74−81.
(11) Denisov, A. Yu.; Noronha, A. M.; Christopher, J. W.; Trempe, J. F.; Pon, R. T; Gehring, K.; Damha, M. J. Solution Structure of an Arabinonucleic Acid (ANA)/RNA Duplex in a Chimeric Hairpin: Comparison with 2′-Fluoro-ANA/RNA and DNA/RNA Hybrids. *Nucleic Acids Res.* **2001**, *29*, 4284−4993.
(12) Kawasaki, A. M.; Casper, M. D.; Freier, S. M.; Lesnik, E. A.; Zounes, M. C.; Cummins, L. L.; Gonzalez, C.; Cook, P. D. Uniformly Modified 2′-Deoxy-2′-fluoro Phosphorothioate Oligonucleotides as Nuclease-Resistant Antisense Compounds with High Affinity and Specificity for RNA Targets. *J. Med. Chem.* **1993**, *36*, 831−841.
(13) Verbeure, B.; Lescrinier, E.; Wang, J.; Herdewijn, P. RNase H Mediated Cleavage of RNA by Cyclohexene Nucleic Acid (CeNA). *Nucleic Acids Res.* **2001**, *29*, 4941−4947.
(14) Cummins, L. L.; Owens, S. R.; Risen, L. M.; Lesnik, E. A.; Freier, S. M.; McGee, D.; Guinosso, C. J.; Cook, P. D. Characterization of Fully 2′-Modified Oligoribonucleotide Hetero- and Homoduplex Hybridization and Nuclease Sensitivity. *Nucleic Acids Res.* **1995**, *23*, 2019−2024.
(15) Demidov, V. V.; Protozanova, E.; Izvolsky, K. I.; Price, C.; Nielsen, P. E.; Frenk-Kamenetskii, M. D. Kinetics and Mechanism of the DNA Double Helix Invasion by Pseudocomplementary Peptide Nucleic Acids. *Proc. Natl. Acad. Sci. U.S.A.* **2002**, *99*, 5953−5958.
(16) Kumar, R.; Singh, S. K.; Koshkin, A. A.; Rajwanshi, V. K.; Meldgaard, M.; Wengel, J. The First Analogues of LNA (Locked Nucleic Acids): Phosphorothioate-LNA and 2′-thio-LNA. *Bioorg. Med. Chem. Lett.* **1998**, *8*, 2219−2222.
(17) Barnes, T. W.; Turner, D. H. C5-(1-Propynyl)-2′-deoxypyrimidines Enhance Mismatch Penalties of DNA: RNA Duplex Formation. *Biochemistry* **2001**, *40*, 12738.
(18) Magat Juan, E. C.; Kondo, J.; Kurihara, T.; Ito, Takanori; Ueno, Y.; Matsuda, A.; Takenaka, A. Crystal Structures of DNA:DNA and DNA:RNA Duplexes Containing 5-(N-Aminohexyl)carbamoyl-Modified Uracils Reveal the Basis for Properties as Antigene and Antisene Molecules. *Nucleic Acids Res.* **2007**, *35*, 1969−1977.
(19) Lesnik, E. A.; Freier, S. M. Relative Thermodynamic Stability of DNA, RNA, and DNA: RNA Hybrid Duplexes: Relationship with Base Composition and Structure. *Biochemistry* **1995**, *34*, 10807−10815.
(20) Noy, A.; Perez, A.; Marquez, M.; Luque, F. J.; Orozco, M. Structure, Recognition Properties, and Flexibility of the DNA·RNA Hybrid. *J. Am. Chem. Soc.* **2005**, *127*, 4910−4920.
(21) Noy, A.; Luque, F. J.; Orozco, M. Theoretical Analysis of Antisense Duplexes: Determinants of the RNase H Susceptibility. *J. Am. Chem. Soc.* **2008**, *130*, 3486−3496.
(22) Priyakumar, U. D.; MacKerell, A. D., Jr. Atomic Detail Investigation of Structure and Dynamics of DNA-RNA Hybrids: A Molecular Dynamics Simulations Study. *J. Phys. Chem. B* **2008**, *112*, 1515−1524.
(23) Nowotny, M.; Gaidamakov, S. A.; Crouch, R. J.; Yang, W. Crystal Structures of RNase H Bound to an RNA/DNA Hybrid: Substrate Specificity and Metal-Dependent Catalysis. *Cell* **2005**, *121*, 1005−1016.
(24) De Vivo, M.; Peraro, M. D.; Klein, M. L. Phosphodiester Cleavage in Ribonuclease H Occurs via an Associative Two-Metal-Aided Catalytic Mechanism. *J. Am. Chem. Soc.* **2008**, *130*, 10955−10962.
(25) Elsasser, B.; Fels, G. Atomic Details of the Associative Phosphodiester Cleavage in Human Ribonuclease H. *Phys. Chem. Chem. Phys.* **2010**, *12*, 11081−11088.
(26) Rosta, E.; Nowotny, M.; Yang, W.; Hummer, G. Catalytic Mechanism of RNA Backbone Cleavage by Ribonuclease H from QM/MM Simulations. *J. Am. Chem. Soc.* **2011**, *133*, 8934−8941.
(27) Jepsen, J. S.; Sorensen, M. D.; Wengel, J. Locked Nucleic Acid: A Potent Nucleic Acid Analog in Therapeutics and Biotechnology. *Oligonucleotides* **2004**, *14*, 130−146.
(28) Kauppinen, S.; Vester, B.; Wengel, J. Locked Nucleic Acid (LNA): High Affinity Targeting of RNA for Diagnostics and Therapeutics. *Drug Discovery Today: Technol.* **2005**, *2*, 287−290.
(29) Vester, B.; Lundberg, L. B.; Sorensen, M. D.; Babu, B. R.; Douthwaite, S.; Wengel, J. LNAzymes: Incorporation of LNA-Type Monomers into DNAzymes Markedly Increases RNA Cleavage. *J. Am. Chem. Soc.* **2002**, *124*, 13682−13683.
(30) Wang, L.; Yang, C. Y. J.; Medley, C. D.; Benner, S. A.; Tan, W. H. Locked Nucleic Acid Molecular Beacons. *J. Am. Chem. Soc.* **2005**, *127*, 15664−15665.
(31) Elmen, J.; Thonberg, H.; Ljungberg, K.; Frieden, M.; Westergaard, M.; Xu, Y. H.; Wahren, B.; Liang, Z. C.; Urum, H.; Koch, T.; Wahlestedt, C. Locked Nucleic Acid (LNA) Mediated Improvements in siRNA Stability and Functionality. *Nucleic Acids Res.* **2005**, *33*, 439−447.
(32) Wahlestedt, C.; Salmi, P.; Good, L.; Kela, J.; Johnsson, T.; Hokfelt, T.; Broberger, C.; Porreca, F.; Lai, J.; Ren, K.; Ossipov, M.; Koshkin, A.; Jakobsen, N.; Skouv, J.; Oerum, H.; Jacobsen, M. H.; Wengel, J. Potent and Nontoxic Antisense Oligonucleotides Containing Locked Nucleic Acids. *Proc. Natl. Acad. Sci. U.S.A.* **2000**, *97*, 5633−5638.
(33) Kloosterman, W. P.; Wienholds, E.; de Bruijn, E.; Kauppinen, S.; Plasterk, R. H. A. In Situ Detection of miRNAs in Animal Embryos Using LNA-Modified Oligonucteotide Probes. *Nat. Methods* **2006**, *3*, 27−29.
(34) Thomsen, R.; Nielsen, P. S.; Jensen, T. H. Dramatically Improved RNA in Situ Hybridization Signals Using LNA-Modified Probes. *RNA* **2005**, *11*, 1745−1748.
(35) Crinelli, R.; Bianchi, M.; Gentilini, L.; Magnani, M. Design and Characterization of Decoy Oligonucleotides Containing Locked Nucleic Acids. *Nucleic Acids Res.* **2002**, *30*, 2435−2443.
(36) Jakobsen, M. R.; Haasnoot, J.; Wengel, J.; Berkhout, B.; Kjems, J. Efficient Inhibition of HIV-1 Expression by LNA Modified Antisense Oligonucleotides and DNAzymes Targeted to Functionally Selected Binding Sites. *Retrovirology* **2007**, *4*, 1−13.
(37) Christiansen, J. K.; Lobedanz, S.; Arar, K.; Wengel, J.; Vester, B. LNA Nucleotides Improve Cleavage Efficiency of Singular and Binary Hammerhead Ribozymes. *Bioorg. Med. Chem.* **2007**, *15*, 6135−6143.
(38) Bonifacio, L.; Church, F. C.; Jarstfer, M. B. Effect of Locked-Nucleic Acid on a Biologically Active G-Quadruplex. A Structure-Activity Relationship of the Thrombin Aptamer. *Int. J. Mol. Sci.* **2008**, *9*, 422−433.
(39) Nielsen, J. T.; Stein, P. C.; Petersen, M. NMR Structure of an α-L-LNA:RNA Hybrid: Structural Implications for RNase H Recognition. *Nucleic Acids Res.* **2003**, *31*, 5858−5867.
(40) Hojland, T.; Veedu, R. N.; Vester, B.; Wengel, J. Enzymatic Synthesis of DNA Strands Containing α-L-LNA (α-L-Configures

Locked Nucleic Acid) Thymine Nucleotides. *Artif. DNA: PNA XNA* **2012**, *3*, 1−8.
(41) Eichert, A.; Behling, K.; Betzel, C.; Erdmann, V. A.; Furste, J. P.; Forster, C. The Crystal Structure of an 'All Locked' Nucleic Acid Duplex. *Nucleic Acids Res.* **2010**, *38*, 6729−6736.
(42) Pande, V.; Nilsson, L. Insights into Structure, Dynamics and Hydration of Locked Nucleic Acid (LNA) Strand-Based Duplexes from Molecular Dynamics Simulations. *Nucleic Acids Res.* **2008**, *36*, 1508−1516.
(43) Nielson, K. M. E.; Petersen, M.; Hakansson, A. E.; Wengel, J.; Jacobsen, J. P. α-L-LNA (α-L-ribo Configured Locked Nucleic Acid) Recognition of DNA: an NMR Spectroscopic Study. *Chemistry* **2002**, *8*, 3001−3009.
(44) Foloppe, N.; MacKerell, A. D., Jr. All-Atom Empirical Force Field for Nucleic Acids: I. Parameter Optimization Based on Small Molecule and Condensed Phase Macromolecular Target Data. *J. Comput. Chem.* **2000**, *21*, 86−104.
(45) MacKerell, A. D., Jr.; Banavali, N. K. All-Atom Empirical Force Field for Nucleic Acids: II. Application to Molecular Dynamics Simulations of DNA and RNA in Solution. *J. Comput. Chem.* **2000**, *21*, 105−120.
(46) Denning, E. J.; Priyakumar, U. D.; Nilsson, L.; MacKerell, A. D., Jr. Impact of 2′-Hydroxyl Sampling on the Conformational Properties of RNA: Update of the CHARMM All-Atom Additive Force Field for RNA. *J. Comput. Chem.* **2011**, *32*, 1929−1943.
(47) Phillips, J. C.; Braun, R.; Wang, Wei; Gumbart, J.; Tajkhorshid, E.; Villa, E.; Chipot, C.; Skeel, R. D.; Kale, L.; Schulten, K. Scalable Molecular Dynamics with NAMD. *J. Comput. Chem.* **2005**, *26*, 1781−1802.
(48) Brooks, B. R.; Brooks, C. L., III; Mackerell, A. D., Jr.; Nilsson, L.; Petrella, R. J.; Roux, B.; Won, Y.; Archontis, G.; Bartels, C.; Boresch, S.; Caflisch, A.; Caves, L.; Cui, Q.; Dinner, A. R.; Feig, M.; Fischer, S.; Gao, J.; Hodoscek, M.; Im, W.; Kuczera, K.; Lazaridis, T.; Ma, J.; Ovchinnikov, V.; Paci, E.; Pastor, R. W.; Post, C. B.; Pu, J. Z.; Schaefer, M.; Tidor, B.; Venable, R. M.; Woodcock, H. L.; Wu, X.; Yang, W.; York, D. M.; Karplus, M. CHARMM: The Biomolecular Simulation Program. *J. Comput. Chem.* **2009**, *30*, 1545−1614.
(49) Ryckaert, J. P.; Ciccotti, G.; Berendsen, H. J. C. Numerical Integration of the Cartesian Equations of Motion of a System with Constraints: Molecular Dynamics of n-Alkanes. *J. Comput. Phys.* **1997**, *23*, 327−341.
(50) Jorgensen, W. L.; Chandrasekhar, J.; Madura, J. D.; Impey, R. W.; Klein, M. L. Potential Functions for Simulating Liquid Water. *J. Chem. Phys.* **1983**, *79*, 926−936.
(51) Field, M. J.; Karplus, M. *CRYSTAL: Program for Crystal Calculations in CHARMM*; Harvard University: Cambridge, MA, 1992.
(52) Darden, T.; Perera, L.; Li, L. P.; Pedersen, L. New Tricks for Modelers from the Crystallography Toolkit: the Particle Mesh Ewald Algorithm and Its Use in Nucleic Acid Simulations. *Structure* **1999**, *7*, R55−R60.
(53) Essmann, U.; Perera, L.; Berkowitz, M. L.; Darden, T. A.; Lee, H.; Pedersen, L. G. A Smooth Particle Mesh Ewald Method. *J. Chem. Phys.* **1995**, *103*, 8577−8593.
(54) Steinbach, P. J.; Brooks, B. R. New Spherical-Cutoff Methods for Long-Range Forces in Macromolecular Simulation. *J. Comput. Chem.* **1994**, *15*, 667−683.
(55) Hoover, W. G. Canonical Dynamics: Equilibrium Phase-Space Distributions. *Phys. Rev. A* **1985**, *31*, 1695−1697.
(56) Feller, S. E.; Zhang, Y.; Pastor, R. W.; Brooks, R. W. Constant Pressure Molecular Dynamics Simulation: the Langevin Piston Method. *J. Chem. Phys.* **1995**, *103*, 4613−4621.
(57) Lavery, R.; Moakher, M.; Maddocks, J. H.; Petkeviciute, D.; Zakrzewska, K. Conformational Analysis of Nucleic Acids Revisited: Curves+. *Nucleic Acids Res.* **2009**, *37*, 5917−5929.
(58) Humphrey, W.; Dalke, A.; Schulten, K. VMD − Visual Molecular Dynamics. *J. Mol. Graphics* **1996**, *14*, 33−38.
(59) Andricioaei, I.; Karplus, M. On the Calculation of Entropy from Covariance Matrices of the Atomic Fluctuations. *J. Chem. Phys.* **2001**, *115*, 6289−6292.
(60) Habtemariam, B.; Anisimov, V. M.; Mackerell, A. D. Cooperative Binding of DNA and CBFβ to the Runt Domain of the CBFα Studied via MD Simulations. *Nucleic Acids Res.* **2005**, *33*, 4212−4222.
(61) Nina, M.; Fonne-Pfister, R.; Beaudegnies, R.; Chekatt, H.; Jung, P. M. J.; Murphy-Kessabi, F.; Mesmaeker, A. D.; Wendeborn, S. Recognition of RNA by Amide Modified Backbone Nucleic Acids: Molecular Dynamics Simulations of DNA-RNA Hybrids in Aqueous Solution. *J. Am. Chem. Soc.* **2005**, *127*, 6027−6038.
(62) Reyes, C. M.; Kollman, P. A. Structure and Thermodynamics of RNA-protein Binding: Using Molecular Dynamics and Free Energy Analysis to Calculate the Free Energies of Binding and Conformational Change. *J. Mol. Biol.* **2000**, *297*, 1145−1158.
(63) Gohlke, H.; Kiel, C.; Case, D. A. Insights into Protein-Protein Binding by Binding Free Energy Calculation and Free Energy Decomposition for the Ras-Raf and Ras-RaIGDS Complexes. *J. Mol. Biol.* **2003**, *330*, 891−913.
(64) Still, W. C.; Tempczyk, A.; Hawley, R. C.; Hendrickson, T. Semi Analytical Treatment of Solvation for Molecular Mechanics and Dynamics. *J. Am. Chem. Soc.* **1990**, *112*, 10606−10614.
(65) Lee, B.; Richards, F. M. The Interpretation of Protein Structures: Estimation of Static Accessibility. *J. Mol. Biol.* **1971**, *55*, 3799−400.
(66) Wengel, J.; Petersen, M.; Frieden, M.; Koch, T. Chemistry of Locked Nucleic Acids (LNA): Design, Synthesis, and Bio-Physical Properties. *Let. Pept. Sci.* **2004**, *10*, 237−253.
(67) Rasmussen, H.; Kastrup, S. J.; Nielsen, J. N.; Nielsen, J. M.; Nielsen, P. E. Crystal Structure of a Peptide Nucleic Acid (PNA) Duplex at 1.7 Å Resolution. *Nat. Struct. Biol.* **1997**, *4*, 98−101.
(68) Schlegel, M. K.; Essen, L. O.; Meggers, E. Duplex Structure of a Minimal Nucleic Acid. *J. Am. Chem. Soc.* **2008**, *130*, 8158−8159.